Recurrent neural network-based Internal Model Control of unknown nonlinear stable systems

Fabio Bonassi[a,*], Riccardo Scattolini[a]

[a]Dipartimento di Elettronica, Informazione e Bioingegneria, Politecnico di Milano, Via Ponzio 34/5, 20133 Milano, Italy - email: name.surname@polimi.it

Abstract

Owing to their superior modeling capabilities, gated Recurrent Neural Networks (RNNs), such as Gated Recurrent Units (GRUs) and Long Short-Term Memory networks (LSTMs), have become popular tools for learning dynamical systems. This paper aims to discuss how these networks can be adopted for the synthesis of Internal Model Control (IMC) architectures. To this end, a first gated RNN is used to learn a model of the unknown input-output stable plant. Then, another gated RNN approximating the model inverse is trained. The proposed scheme is able to cope with the saturation of the control variables, and it can be deployed on low-power embedded controllers since it does not require any online computation. The approach is then tested on the Quadruple Tank benchmark system, resulting in satisfactory closed-loop performances.

Keywords: Recurrent Neural Network, Internal Model Control, Neurocontrollers

1. Introduction

In recent years, Neural Networks (NNs) have gained popularity in the control systems community. The key factors behind this success are the flexibility and modeling power of these tools, which make them suitable for system identification [1, 2] and control tasks [3, 4].

Through the control system designer lenses, the wide variety of neural networks' architectures can be classified in Feed-Forward Neural Networks (FFNNs), and Recurrent Neural Networks (RNNs) [5]. The former group is composed of static NNs, which do not have inherent memory and are mainly used to approximate static functions, for which task they enjoy universal approximation capabilities [6]. On the contrary, RNNs are stateful NNs, i.e., they retain memory of the past data, and hence they are particularly suitable for learning timeseries and dynamical systems [7, 8, 9]. In these tasks, RNNs have been shown to feature universal approximation capabilities [10].

Among RNNs, the most popular architectures are the so-called gated recurrent networks, designed to avoid the vanishing/exploding gradient problems, which instead plague traditional RNN architectures [11]. More specifically, Gated Recurrent Units

---

*Corresponding author

(GRUs) [12] and Long Short-Term Memory (LSTM) [13] are acknowledged to be the go-to architectures for system identification tasks [1].

Owing to their modeling capabilities, NNs have been widely adopted in conjunction with model-based control strategies. For example, the use of RNNs as system models for Model Predictive Control (MPC) design has been widely explored both in the industry [14, 15, 16], and in the academia [17, 18, 19, 20].

An alternative control architecture in which NNs can be profitably employed is the Internal Model Control (IMC) scheme. This architecture is particularly interesting because of its limited online computational cost, which makes it suitable to the deployment to low-power embedded controllers. In the IMC scheme, a reliable model of the (unknown) plant is assumed to be available, and the controller is constructed as the inverse (or, at least, an approximation of the inverse) of such model [21]. Hence, this controller is supposed to generate the control action that steers the model output close to the reference trajectory. In order to avoid open-loop operations, the plant-model mismatch is fed back and summed to the reference signal [21, 22], thus leveraging the output measurement to improve the robustness of the scheme.

This paper aims to show how the modeling capabilities of RNNs can be exploited to synthesize the ingredients of the IMC scheme. More specifically, we propose using a GRU network as the plant's model and then learning a controller GRU network as an approximation of the model's inverse itself. The idea of using NNs for IMC design is not totally new. Indeed, a similar approach was proposed in [23], where however static FFNNs were used as the system's model and model's inverse approximation. Analogously, in [24] FFNNs were used in an auto-regressive configuration to control a stable SISO system.

While these papers inspired the present work, we believe that RNNs represent better candidates for learning the model and its inverse. First, gated recurrent networks naturally retain long-term memory of the past trajectories. In contrast, for feed-forward auto-regressive architectures, this memory must be enforced by supplying the past input-output data-points as inputs of the network [24], typically resulting in less accurate long-term learning compared to RNNs [25]. Secondly, since the controller is implemented by a gated recurrent network, which is inherently strictly proper, the issue of the controller's improperness discussed in [24] does not arise. Finally, owing to the model and controller learning procedures, the proposed scheme only needs the system to be input-output stable and, differently from other works, it is not required to be SISO. The proposed controller also accounts for input saturation constraints. The clear advantages of using gated recurrent networks come, however, at the expense of losing the guarantees on the existence of the exact model's inverse. Nonetheless, we show that a sufficiently accurate approximation of this inverse is enough to ensure closed-loop stability and satisfactory performances.

Under the assumption of input-output stability of the plant to be controlled, we propose to enforce a similar stability property for the learned system model, namely the Incremental Input-to-State Stability (δISS) [26]. In brief, this property guarantees that asymptotically the effects of different initial conditions vanish and the smaller the maximum euclidean distance between two input sequences, the closer are the resulting state (and output) trajectories. The consequences of this property are herein leveraged to guarantee the closed-loop stability, and to ease the generation of the dataset used

to learn the controller network. For this purpose, note that sufficient conditions to guarantee the δISS of several gated RNNs, such as LSTMs [19, 27] and GRUs [28, 29], have been recently proposed in the literature. These conditions can be easily enforced during the network training procedure.

The proposed approach has been tested on the Quadruple Tank system described in [30]. In particular, after showing how a stable gated recurrent network can be used to learn the plant's model, we focus on the problem of generating a suitable dataset for the controller learning procedure. The closed-loop performances have been eventually tested, turning out to be satisfactory.

The paper is structured as follows. In Section 2 state-space RNNs are presented, with a particular focus on deep GRUs, for which recent stability results for these systems are summarized. Then, in Section 3, the IMC scheme is described, and we show how to use GRUs to learn the model of the system and to approximate its inverse to obtain the controller. Traditional stability results of IMC are summarized in Section 4. In Section 5 the application of the proposed approach is described on the Quadruple Tank benchmark system, and the closed-loop performances are assessed. Eventually, conclusions are drawn in Section 6.

1.1. Notation

For vector v, we denote by v' its transpose and by $\|v\|$ its Euclidean norm. Sequences of vectors are represented using boldface fonts, i.e. $\boldsymbol{v} = \{v(0), v(1), ...\}$. With a slight abuse of notation, we denote $\|\boldsymbol{v}\|_p = \max_{k \geqslant 0} \|v(k)\|_p$. With reference to time-varying quantity $x(k)$, unless otherwise specified the generic time index k may be omitted, i.e. $x = x(k)$, and superscript $^+$ may be used to indicate the same quantity at time $k+1$, i.e. $x^+ = x(k+1)$. The symbol $\circ$ denotes the Hadamard (element-wise) product between matrices. The sigmoid and tanh activation functions are indicated by σ and ϕ, respectively, i.e. $\sigma(x) = \frac{1}{1+e^{-x}}$ and $\phi(x) = \tanh(x)$.

2. Recurrent neural networks

This section aims to introduce recurrent networks and show how they can be employed to learn nonlinear dynamical systems. As discussed, since RNNs are stateful neural networks, they are well-suited to the system identification task since the memory of the past data is encoded in the states of the network. In this work we consider gated recurrent network such as GRUs [28] and LSTMs [19, 27]. In these architectures, the gates manage the flow of information throughout the network, thus avoiding the so-called vanishing and exploding gradient problems [31]. A generic gated recurrent network in state-space form reads as

$$\begin{cases} \xi^+ = f(\xi, v, \Phi) \\ \zeta = g(\xi, \Phi) \end{cases}, \tag{1}$$

where $\xi \in \mathbb{R}^n$ is the state vector, $v \in \mathbb{R}^m$ is the input, $\zeta \in \mathbb{R}^p$ is the output, and Φ is the set of parameters. The goal of the learning procedure is to find the parametrization Φ which best explains the available data. For example, in a system identification task, one

wants the RNN to reproduce the measured output trajectory $\boldsymbol{y}$ given the input sequence $\boldsymbol{u}$ applied to the plant.

For the sake of simplicity, the reminder of this work makes reference to GRU networks, but the approach can be easily extended to LSTM architectures [19].

2.1. Deep GRU architecture

In the following, the architecture of deep Gated Recurrent Units is described in detail. Let us indicate by M be the number of layers of the network. We denote by $\xi^i \in \mathbb{R}^{n_i}$ and $v^i \in \mathbb{R}^{m_i}$ the state and the input of the i-th layer, respectively. The state equation of the layer $i \in \{1, ..., M\}$ reads as

$$\xi^{i,+} = z^i \circ \xi^i + (1 - z^i) \circ \phi(W_r^i v^i + U_r^i f^i \circ \xi^i + b_r^i), \tag{2a}$$

where $z^i = z^i(\xi^i, v^i)$ and $f^i = f^i(\xi^i, v^i)$ are the update and forget gates, defined as

$$z^i(\xi^i, v^i) = \sigma(W_z^i v^i + U_z^i \xi^i + b_z^i), \tag{2b}$$

$$f^i(\xi^i, v^i) = \sigma(W_f^i v^i + U_f^i \xi^i + b_f^i). \tag{2c}$$

$W_\star^i$, $U_\star^i$, and $b_\star^i$ are the weight matrices of the layer. As far as v_i is concerned, the input to the first layer is the network's input, i.e. $v_1 = v$, while the input of any following layer is the updated state of the previous one, which means

$$\begin{cases} v^1 = v \\ v^i = \xi^{i-1,+} \quad \forall i \in \{2, ..., M\} \end{cases}. \tag{2d}$$

Eventually, the following output transformation is applied

$$\zeta = g(U_o \xi^M + b_o), \tag{2e}$$

where g may be a nonlinear activation function, such as σ and ϕ, or – if (2e) is linear – the identity function. The set of weights Φ of the deep GRU is

$$\Phi = \left\{ \{W_z^i, U_z^i, b_z^i, W_r^i, U_r^i, b_r^i, W_f^i, U_f^i, b_f^i\}_{\forall i \in \{1, ..., M\}}, U_o, b_o \right\}.$$

It is worth noticing that, collecting the states ξ^i in a vector $\xi = [\xi^{1\prime}, ..., \xi^{M\prime}]'$, the deep GRU model (2) falls in the nonlinear state-space form (1).

2.2. Stability properties

We now summarize few stability results concerning deep GRUs that will be useful in the remainder of the article. For more details, the interested reader is addressed to [28]. In the interests of clarity, in the following, we denote by $\xi(k)$ the state trajectory of the deep GRU at time k, obtained initializing (2) in some initial state $\bar{\xi}$ and applying the input sequence $\boldsymbol{v}$.

4

Lemma 1. *The set $\Xi = [-1,1]^n = \times_{i=1}^{M}[-1,1]^{n_i}$ is an invariant set of the deep GRU* (2)*, i.e. for any input v*

$$\xi(k) \in \Xi \implies \xi(k+1) \in \Xi.$$

Lemma 2. *For any initial state $\bar{\xi} = [\bar{\xi}^{1\prime}, ..., \bar{\xi}^{M\prime}]^{\prime}$ and any input sequence $\boldsymbol{v}$, it holds that*

  i. *if $\bar{\xi} \notin \Xi$, $\|\xi(k)\|_{\infty}$ is strictly decreasing until $\xi(k) \in \Xi$,*

 ii. *the convergence happens in finite time, i.e. $\exists \bar{k} \geqslant 0$ finite such that $\xi(k) \in \Xi$ for any $k \geqslant \bar{k}$,*

iii. *the convergence of each component of ξ into $[-1,1]$ is exponential.*

We remind that a function $\Psi(s)$ is of class $\mathcal{K}_{\infty}$ if it is monotonically increasing, $\Psi(0) = 0$, and $\Psi(s) \to \infty$ if $s \to \infty$. Similarly, $\Psi(s,t)$ is of class $\mathcal{KL}$ if it is $\mathcal{K}_{\infty}$ with respect to s and $\Psi(s,t) \to 0$ when $t \to \infty$. The following stability-like notions can hence be formalized.

Definition 1 (GAS). *System* (1) *is said to be Globally Asymptotically Stable (GAS) if there exist $\beta \in \mathcal{KL}$ such that for any initial condition $\bar{\xi}$ and any k*

$$\|\xi(k,\bar{\xi},0)\| \leqslant \beta(\|\bar{\xi}\|, k), \tag{3}$$

where $\xi(k,\bar{\xi},\boldsymbol{v})$ is the state trajectory obtained initializing system (1) *in $\bar{\xi}$ and feeding it with the input sequence $\boldsymbol{v}$.*

Note that (3) implies that, for any initial state, the autonomous system underlying (1) converges to the origin.

Definition 2 (δISS). *System* (1) *is Incrementally Input-to-State Stable (δISS) if there exists functions $\beta \in \mathcal{KL}$ and $\gamma_v \in \mathcal{K}_{\infty}$ such that for any pair of initial conditions $\bar{\xi}_a$ and $\bar{\xi}_b$, any pair of input sequences $\boldsymbol{v_a} \in V$ and $\boldsymbol{v_b} \in V$, and any k*

$$\|\xi_a(k,\bar{\xi}_a,\boldsymbol{v}_a) - \xi_b(k,\bar{\xi}_b,\boldsymbol{v}_b)\| \leqslant \beta(\|\bar{\xi}_a - \bar{\xi}_b\|, k) + \gamma_v(\|\boldsymbol{v}_a - \boldsymbol{v}_b\|), \tag{4}$$

where $\xi_*(k,\bar{\xi}_*,\boldsymbol{v}_*)$ denotes the state trajectory of (1)*, initialized in $\bar{\xi}_*$ and fed with $\boldsymbol{v}_*$.*

Remarkably, the δISS property implies that the effects of initial conditions asymptotically vanish, so that the modeling performances are independent of the initialization. Moreover, the δISS entails that the distance between the state trajectories produced by two different input sequences, $\boldsymbol{v}_a$ and $\boldsymbol{v}_b$, is bounded by a function $\gamma_v(\|\boldsymbol{v}_a - \boldsymbol{v}_b\|)$, which is strictly increasing with the maximum distance between the two inputs. Hence, the closer the input sequences, the closer the resulting state trajectories. Lastly, it is worth noticing that if the system is δISS it is also GAS.

In the following, we customarily assume that the input of the network is bounded in $V = [-1,1]^m$, see [5]. Then, the following Theorem from [28] provides a sufficient condition that guarantees the δISS of the deep GRU, in terms of its parametrization Φ.
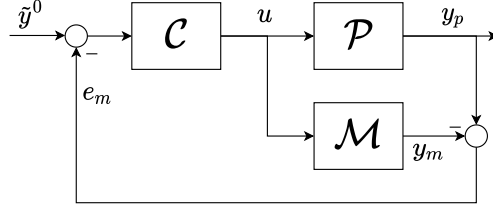
Figure 1: General scheme of IMC.

Theorem 1. *The deep GRU network* (2) *is δISS if, for each layer* $i \in \{1, ..., M\}$, *the weights satisfy the following condition*

$$\|U_r\|_\infty \left(\frac{1}{4} \|U_f\|_\infty + \bar{\sigma}_f \right) < 1 - \frac{1}{4} \frac{1 + \bar{\phi}_r}{1 - \bar{\sigma}_z} \|U_z\|_\infty, \tag{5}$$

where

$$\bar{\sigma}_z = \sigma(\|W_z \quad U_z \quad b_z\|_\infty), \tag{6a}$$

$$\bar{\sigma}_f = \sigma(\|W_f \quad U_f \quad b_f\|_\infty), \tag{6b}$$

$$\bar{\phi}_r = \phi(\|W_r \quad U_r \quad b_r\|_\infty). \tag{6c}$$

3. Internal model control architecture

Having introduced GRUs and their stability properties, we can now discuss how they can be suitably employed in the Internal Model Control structure. The IMC scheme, depicted in Figure 1, features three blocks: the unknown plant $\mathcal{P}$, its model $\mathcal{M}$, and the controller $\mathcal{C}$. The plant $\mathcal{P}$ is assumed to be input-output stable, and it is described by the following (unknown) state-space dynamical system

$$\mathcal{P} : \begin{cases} x^+ = f_p(x, u) \\ y_p = g_p(x) \end{cases}. \tag{7}$$

For compactness, we denote by $y_p(k, \bar{x}, \boldsymbol{u})$ the output trajectory of (7), initialized in $\bar{x}$ and fed with the input sequence $\boldsymbol{u}$.

Ideally, one wants the system's model $\mathcal{M}$ to perfectly match $\mathcal{P}$ from an input-output perspective. This means that, letting $y_m(k, \bar{\xi}_m, \boldsymbol{u})$ be the output trajectory of $\mathcal{M}$ initialized in the state $\bar{\xi}_m$ and fed with the input sequence $\boldsymbol{u}$, then $\mathcal{M} \equiv \mathcal{P}$ if, for any $\boldsymbol{u}$ and any $\bar{x}$, there exists an initial state $\bar{\xi}_m$ such that $y_p(k, \bar{x}, \boldsymbol{u}) = y_m(k, \bar{\xi}_m, \boldsymbol{u})$, for any $k \geqslant 0$.

The controller block $\mathcal{C}$ is, ideally, the inverse of the model $\mathcal{M}$. This implies that, for any output reference trajectory $\tilde{\boldsymbol{y}}^0$, and for any initial condition of the model $\bar{\xi}_m$, there exists an initial state of the controller $\bar{\xi}_c$ such that the control action generated by $\mathcal{C}$ steers the model output to the reference trajectory. More formally, this condition reads
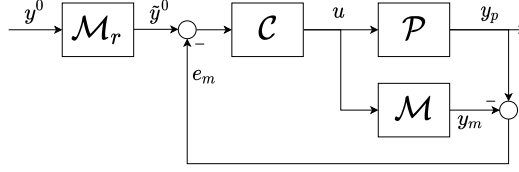
Figure 2: General scheme of IMC with model reference.

as $y_m(k, \bar{\xi}_m, u_c(k, \bar{\xi}_c, \tilde{\boldsymbol{y}}^0)) = \tilde{\boldsymbol{y}}^0$ for any $k \geqslant 0$, where $u = u_c(k, \bar{\xi}_c, \tilde{\boldsymbol{y}}^0)$ denotes the output of the controller $\mathcal{C}$ when initialized in $\bar{\xi}_c$ and fed with $\tilde{\boldsymbol{y}}^0$.

In practice, however, $\mathcal{C}$ is synthesized as an approximation of the model inverse, since the exact inverse may be not proper, not analytically defined, or even not stable [22]. Moreover, since a plant-model mismatch may be present, the IMC scheme depicted in Figure 1 features the modeling error feedback $e_m = y_p - y_m$, see again [22].

In the following we consider a model $\mathcal{M}$ learned by a GRU network, and we discuss how a GRU resembling the model's inverse can be trained and used as controller $\mathcal{C}$. Moreover, in the reminder of this work we consider the modified control scheme depicted in Figure 2, where a model reference block $\mathcal{M}_r$ has been added [24]. This block encodes the desired closed-loop response to the reference signal y^0. Indeed, when the IMC control is perfect (i.e. $y_p = \tilde{y}^0$), the relationship between the reference signal y^0 and the system output y_p is exactly the reference model $\mathcal{M}_r$.

3.1. System model identification

As discussed, the system model $\mathcal{M}$ is required to implement the IMC architecture. A system identification procedure is hence required to retrieve a gated recurrent network that approximates the unknown plant. Such network takes the following form

$$\mathcal{M} : \begin{cases} \xi_m^+ = f_m(\xi_m, u, \Phi_m) \\ y_m = g_m(\xi_m, \Phi_m) \end{cases}. \tag{8a}$$

More specifically, the recurrent architecture here considered is a GRU in the form of (2), with a linear output transformation

$$g_m(\xi_m, \Phi_m) = U_{o,m}\, \xi_m^M + b_m, \tag{8b}$$

where ξ_m^M The input of the model is the control action applied to the plant, u, and its output is y_m, desirably close to the plant's output y_p. It is customarily assumed that u and y_m are normalized, i.e. they lie in the range $[-1, 1]$.

The learning procedure consists in finding the parametrization Φ_m^* which minimizes the simulation error $y_m(k, \bar{\xi}_m, \boldsymbol{u}) - y_p(k, \bar{x}, \boldsymbol{u})$, ideally for any possible input sequence $\boldsymbol{u}$. In practice, one performs a limited number of experiments on the unknown plant, and collects N_s input-output sequences from the unknown plant, denoted by $(\boldsymbol{u}^{\{i\}}, \boldsymbol{y}_p^{\{i\}})$, $i \in \{1, ..., N_s\}$. Note that any sequence i, with length $T_s^{\{i\}}$, may describe an experiment, or it may be obtained via the Truncated Back-Propagation Through

7

Time (TBPTT) [7]. In essence, TBPTT consists in extracting partially overlapping sub-sequences from a longer one, and it allows to significantly improve the performances of the trained network by artificially enlarging the dataset [7].

As discussed, the plant $\mathcal{P}$ is assumed to be input-output stable. Therefore, to ensure the consistency of the model to the plant, the stability of the model $\mathcal{M}$ is enforced. We point out that the δISS property discussed in Section 2 implies the input-output stability of the model, since the output transformation is simply a static transformation. The condition stated in Theorem 1 is thus leveraged during the training procedure to ensure the stability of $\mathcal{M}$. Since most training algorithms are unconstrained, condition (5) is relaxed by penalizing its violation in the loss function, as discussed in [28]. Hence, at any iteration of the training algorithm, the loss function L_m – defined over a batch $\mathcal{I}$, that is, a random subset of sequences – is minimized. The loss function considered reads as

$$L_m = \sum_{i \in \mathcal{I}} \mathrm{MSE}(y_m(k, \bar{\xi}_m, \boldsymbol{u}^{\{i\}}), \boldsymbol{y}_p^{\{i\}}) + \sum_{j=1}^{M} \rho(\nu^j), \tag{9}$$

where

$$\mathrm{MSE}(\boldsymbol{y}_m, \boldsymbol{y}_p^{\{i\}}) = \frac{1}{T_s^{\{i\}} - T_w} \sum_{k=T_w}^{T_s^{\{i\}}} \left\| y_m(k) - y_p^{\{i\}}(k) \right\|^2. \tag{10}$$

The first term in L_m corresponds to the Mean Square Error (MSE) between the the measured output $\boldsymbol{y}_p^{\{i\}}$ and the model's open-loop prediction $y_m(k, \bar{\xi}_m, \boldsymbol{u}^{\{i\}})$, obtained initializing (7) in the random initial state $\bar{\xi}_m$ and applying the input sequence $\boldsymbol{u}^{\{i\}}$. Note that the output error is not penalized in the first T_w steps, known as the washout period, to accommodate the initial transitory associated with the random initialization of the model. The second term of (9) penalizes the violation of the stability condition (5) for each layer $i \in \{1, ..., M\}$, i.e.

$$\nu^j = \|U_r\|_\infty \left(\frac{1}{4} \|U_f\|_\infty + \bar{\sigma}_f \right) + \frac{1}{4} \frac{1 + \bar{\phi}_r}{1 - \bar{\sigma}_z} \|U_z\|_\infty - 1, \tag{11}$$

by means of a monotonically increasing function ρ, see [28]. Any training algorithm, such as SGD, Adam, or RMSProp, can be then used to train (7), i.e. to retrieve a parametrization Φ_m^* for which the model is suitably accurate [5]. In the following, we assume that the model $\mathcal{M}$ has been trained and validated, and that Theorem 1 holds, so that the model is stable.

3.2. Controller learning

Having an accurate model of the plant, according to the IMC paradigm, one should now find the right-inverse of the model, which, with a slight abuse of notation, will be denoted by $\mathcal{M}^{-1}$. Due to the complexity of gated recurrent networks, retrieving an analytical expression of $\mathcal{M}^{-1}$ may not be possible, and its existence may not even be guaranteed.

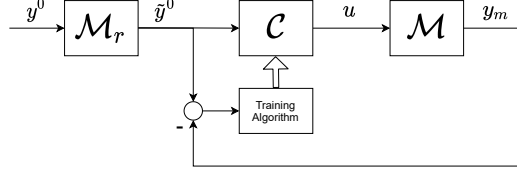For this reason, the following gated recurrent network, which approximates the

Figure 3: Scheme of the controller's learning.

model inverse, is considered

$$\mathcal{C} : \begin{cases} \xi_c^+ = f_c(\xi_c, \tilde{y}^0, \Phi_c) \\ u_c = g_c(\xi_c, \Phi_c) \end{cases}, \tag{12a}$$

where the input of the controller is the reference trajectory $\tilde{y}^0$ that should be tracked by the IMC scheme, obtained filtering the set-point y^0 with the model reference $\mathcal{M}_r$, see Figure 2. The state of the controller is ξ_c, and its output is the control signal applied to the system, denoted by u_c. In this paper, we assume that also $\mathcal{C}$ is learned by a GRU network described by (2), with output transformation

$$g_c(\xi_c, \Phi_c) = \phi(U_{o,c}\,\xi_c^M + b_{o,c}), \tag{12b}$$

where ξ_c^M is the state of the last GRU layer.

To train the controller, we adopt the learning procedure depicted in Figure 3, similar to the procedures proposed in [23, 24]. The goal is to find the parametrization Φ_c such that the input signal u_c generated by the network steers the model's output y_m as close as possible to the reference $\tilde{y}^0$. It is worth noticing that, at this stage, the system model has been already identified, and hence its weights Φ_m^* are fixed.

The dataset used for the controller's training, which consists of a set of reference signals $\tilde{y}^0$ that the controller learns to track, is synthetically produced by generating an arbitrarily large number of suitable set-points y^0, which are then filtered with the selected model reference $\mathcal{M}_r$. The closer these references are to those imposed in closed-loop system operation, the more accurate the controller action will be. Note that the generated references should be feasible for the model, meaning that, at least asymptotically, the difference between the filtered reference $\tilde{y}^0$ and the model output y_m can be made arbitrarily small through a suitable tuning of Φ_c. This means that, for example, the reference may settle to the steady-state value $\tilde{y}_s^0$ only if such set-point is associated to a feasible equilibrium of the model, i.e. if there exists a feasible input $u_s \in [-1, 1]^m$ and a state $\xi_s \in \Xi$ such that $\mathcal{M}$ admits $(u_s, \xi_s, \tilde{y}_s^0)$ as an equilibrium. This problem is further discussed in Section 5.

Moreover, since the $\tanh$ activation function is used in the output transformation (12b), the controller's output u_c is guaranteed to lie in $[-1, 1]^m$. This reflects the assumption that u_c is normalized in such a way that it is unity-bounded, as discussed in Section 3.1. Other output activation functions, such as the saturation, can however be adopted.

9

The training procedure of the controller $\mathcal{C}$ is carried out as follows. First, an arbitrarily large amount of suitable reference signals, denoted by $\boldsymbol{y}^{0,\{i\}}$, are generated. Then, they are filtered with the model reference $\mathcal{M}_r$ to obtain $\tilde{\boldsymbol{y}}^{0,\{i\}}$. At each training epoch, these sequences are randomly divided in batches, and the loss function L_c is minimized over each batch $\mathcal{I}$. In particular, the loss function is stated as

$$L_c = \sum_{i \in \mathcal{I}} \mathrm{MSE}\Big(y_m(k, \bar{\xi}_m, u_c(k, \bar{\xi}_c, \tilde{\boldsymbol{y}}^{0,\{i\}})), \tilde{\boldsymbol{y}}^{0,\{i\}}\Big) + \sum_{j=1}^{M} \rho(\nu^j), \tag{13}$$

where the first term is the MSE between the reference trajectory $\tilde{y}^0$ and the model's output y_m, when $\mathcal{M}$ is initialized in the random state $\bar{\xi}_m$ and is fed with the control action u_c generated by $\mathcal{C}$, see Figure 3. In other words, this term penalizes the nominal output tracking error, while the second term, as discussed in Section 3.1, allows to fulfill the δISS condition (5).

The training algorithm is thus used to train (12), retrieving the controller's weights Φ_c^* that make the output tracking error over the validation dataset sufficiently small.

At this stage, the control system has been entirely learned from the data. In the following Section the stability properties of the proposed control scheme are discussed.

4. Stability properties

Owing to its particular structure, the IMC scheme enjoys the following closed-loop properties [23].

Property 1 (Stability [21]). *If the plant and the controller are input-output stable and the model is exact, the closed-loop system is input-output stable.*

Note that, in absence of output noise, if $\mathcal{M} = \mathcal{P}$ the modeling error feedback is null, i.e. $e_m = 0$, and the IMC controller operates in open-loop. Thus, if $\mathcal{C}$ and $\mathcal{P}$ are input-output stable, the overall scheme is input-output stable as well. A δISS controller, trained as discussed in Section 3.2, is hence able to guarantee the closed-loop stability.

Property 2 (Perfect Control [21]). *Assume that the plant is input-output stable, that the model is exact, and that the controller matches the model's inverse, i.e. $\mathcal{C} = \mathcal{M}^{-1}$. Then, if $\mathcal{C}$ is input-output stable, the closed-loop is input-output stable and matches the model reference $\mathcal{M}_r$.*

Indeed, under the assumption of exact model availability, the control system operates in open-loop. Since $\mathcal{C} = \mathcal{M}^{-1} = \mathcal{P}^{-1}$, it holds that $y_p = \tilde{y}^0$, and hence the relationship between y^0 and y_p is the model reference $\mathcal{M}_r$.

Property 3 (Zero Offset [21]). *Assume that the plant is input-output stable, that the model is exact and admits an inverse, and that the steady state control action generated by the controller matches the steady-state value of the model's inverse. Then, if the controller is input-output stable, offset-free tracking is asymptotically attained.*

This last property means that, owing to the stability of $\mathcal{M}$ and $\mathcal{C}$, if the controller matches the inverse operator of the model – at least at steady state –, then $y_m(k, \bar{\xi}_m, u_c(k, \bar{\xi}_c, \tilde{y}^0)) \xrightarrow[k \to \infty]{} \tilde{y}^0(k)$, i.e. offset-free control is achieved.

While these properties are remarkable, in practice it is very hard to guarantee the absence of a plant-model mismatch and the exactness of the model's inverse. In the following, we thus show the closed-loop input-output stability in non-ideal cases, where $\mathcal{M}$ is not exact and $\mathcal{C}$ does not match the model's inverse.

Proposition 1. *Assume that the plant $\mathcal{P}$ can be described by the equations of the model $\mathcal{M}$ with a fictitious additive disturbance d, which accounts for the plant-model mismatch*

$$\mathcal{P}: \begin{cases} x^+ = f_m(x, u, \Phi_m^*) \\ y_p = g_m(x, \Phi_m^*) + d \end{cases}. \tag{14}$$

Then, if the model $\mathcal{M}$ and the controller $\mathcal{C}$ are δISS, the closed-loop IMC scheme depicted in Figure 2 is input-output stable with respect to the reference trajectory $\tilde{\boldsymbol{y}}^0$.

Proof. Owing to Lemma 2, and in light of the output transformation of $\mathcal{C}$ defined in (12), the control variable u is unity-bounded, i.e. $u(k) \in [-1, 1]^m$. Therefore, since both $\mathcal{P}$ and $\mathcal{M}$ are stable, then y_p, y_m and d are bounded. Hence the system is input-output stable. ∎

It is worth noticing that the modeling error feedback e_m, defined as

$$e_m(k) = y_p(k, \bar{x}, \boldsymbol{u}) - y_m(k, \bar{\xi}_m, \boldsymbol{u}), \tag{15}$$

is asymptotically bounded. In fact, owing to the δISS of $\mathcal{M}$, the effect of the wrong initialization of the model asymptotically vanishes, so that e_m converges to the (bounded) disturbance d that represents the plant-model mismatch.

5. Numerical example

5.1. Benchmark description

The performances of the proposed control scheme have been assessed on the Quadruple Tank system reported in [30]. The system, depicted in Figure 4, consists in four tanks containing water, whose levels are denoted by h_1, h_2, h_3, and h_4, which are fed with two controllable pumps. Specifically, two triple valves split the flow rate q_a in $q_1 = \gamma_a q_a$ and $q_3 = (1 - \gamma_a)q_a$, and the flow rate q_b in $q_2 = \gamma_b q_b$ and $q_4 = (1 - \gamma_b)q_b$. The equations of the system are

$$
\begin{aligned}
\dot{h}_1 &= -\frac{a_1}{S}\sqrt{2gh_1} + \frac{a_3}{S}\sqrt{2gh_3} + \frac{\gamma_a}{S}q_a, \\
\dot{h}_2 &= -\frac{a_2}{S}\sqrt{2gh_2} + \frac{a_4}{S}\sqrt{2gh_4} + \frac{\gamma_b}{S}q_b, \\
\dot{h}_3 &= -\frac{a_3}{S}\sqrt{2gh_3} + \frac{1 - \gamma_b}{S}q_b, \\
\dot{h}_4 &= -\frac{a_4}{S}\sqrt{2gh_4} + \frac{1 - \gamma_a}{S}q_a,
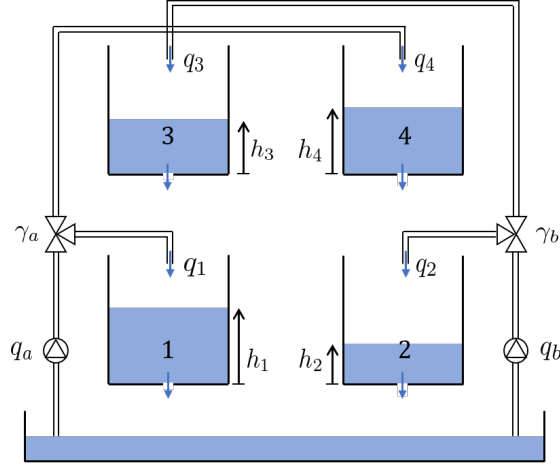\end{aligned} \tag{16a}
$$

11

Figure 4: Quadruple tank system [28]

Table 1: Benchmark system parameters

Parameter	Value	Units	Parameter	Value	Units
a_1	$1.31 \cdot 10^{-4}$	m^2	$[h_1^{min}, h_1^{max}]$	$[0, 1.36]$	m
a_2	$1.51 \cdot 10^{-4}$	m^2	$[h_2^{min}, h_2^{max}]$	$[0, 1.36]$	m
a_3	$9.27 \cdot 10^{-5}$	m^2	$[h_3^{min}, h_3^{max}]$	$[0, 1.3]$	m
a_4	$8.82 \cdot 10^{-5}$	m^2	$[h_4^{min}, h_4^{max}]$	$[0, 1.3]$	m
S	0.06	m^2	$[q_a^{min}, q_a^{max}]$	$[0, 9 \cdot 10^{-4}]$	$\frac{m^3}{s}$
γ_a	0.3		$[q_b^{min}, q_b^{max}]$	$[0, 1.3 \cdot 10^{-3}]$	$\frac{m^3}{s}$
γ_b	0.4				

where the parameters of the system have been reported in Table 1. The water levels, as well as the control variables, are also subject to saturation limits

$$
\begin{aligned}
h_i &\in [h_i^{min}, h_i^{max}] \quad \forall i \in \{1, ..., 4\}, \\
q_a &\in [q_a^{min}, q_a^{max}], \\
q_b &\in [q_b^{min}, q_b^{max}].
\end{aligned}
\tag{16b}
$$

In the following it is assumed that only h_1 and h_2 are measurable, i.e. the output of the system is $y_p = [h_1, h_2]'$, while the input of the system is $u = [q_a, q_b]'$. The control goal is to steer the system's output y_p to the reference y^0 mimicking the response of the reference model $\mathcal{M}_r$.

As discussed in Section 3, the synthesis of an IMC regulator is articulated in the following steps: *(i)* learning a model $\mathcal{M}$ of the system; *(ii)* generating a dataset of feasible reference trajectories; *(iii)* learning a controller $\mathcal{C}$ which approximates the model's inverse.
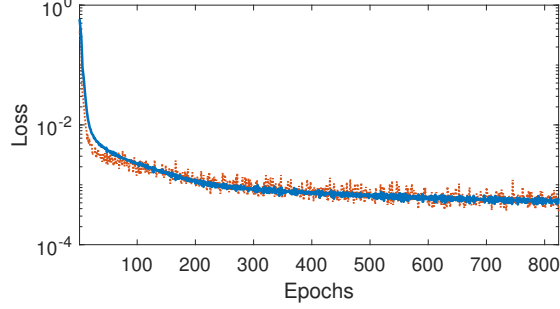
Figure 5: Model training: evolution of the average loss function across all the batches (blue line) and MSE on the validation dataset (red dotted line).

5.2. Model training

The Quadruple Tank system described by (16) has been implemented in MATLAB. In order to retrieve the data required for the model's training, the system has been fed with Multilevel Pseudo-Random Signals (MPRS) as inputs to properly excite the system and collect data in a broad operating region. According to the TBPTT paradigm, $N_s = 200$ random partially-overlapping sequences have been extracted from the experiment. Each pair of input-output sequences $(\boldsymbol{u}^{\{i\}}, \boldsymbol{y}^{\{i\}})$ is made by $T_s^{\{i\}} = 700$ data-points, collected with a sampling time $\tau_s = 25s$. The data has been suitably normalized, so that (16b) translates into the unity-boundedness of y_p and u.

A deep GRU with $M = 2$ layers, made by $n_i = 10$ units each, has been used to learn the system model. The training procedure discussed in Section 3.1 has been carried out with TensorFlow 1.15 on Python 3.7, using the RMSProp [5] as optimizer. It is worth recalling that the δISS property has been enforced by penalizing the violation of the δISS condition (11). This is achieved using a piece-wise linear cost $\rho(\nu^i)$ which steers ν^i, $i \in \{1, ..., M\}$, to some sufficiently small negative value, see [28].

At each training epoch, the set of N_s sequences is randomly split into several batches, with respect to which the optimizer tunes the network's parameters. After each epoch, the performances of the network have been evaluated on 25 validation sequences extracted from an independent experiment. The network training was halted when the model's performance on the validation set stopped improving, thus obtaining the model's weights Φ_m^*.

The evolution of the loss function is shown in Figure 5. Overall, the training procedure took 823 epochs. Eventually, the modeling performances have been tested on an independent test sequence, leading to the satisfactory results depicted in Figure 6. These performances have also been quantified using the so-called FIT index [%], defined as

$$\text{FIT} = 100\left(1 - \sqrt{\frac{\text{MSE}(y_m(k, \bar{\xi}_m, \boldsymbol{u}^{\{ts\}}), \boldsymbol{y}^{\{ts\}})}{\text{MSE}(\boldsymbol{y}^{\{ts\}}, y_{avg}^{\{ts\}})}}\right), \tag{17}$$

where $(\boldsymbol{u}^{\{ts\}}, \boldsymbol{y}^{\{ts\}})$ is the test sequence, $y_{avg}^{\{ts\}}$ the output average value, and y_m the corresponding model's open-loop prediction. The trained model scores $FIT = 96.5\%$, which indicates remarkable modeling performances.
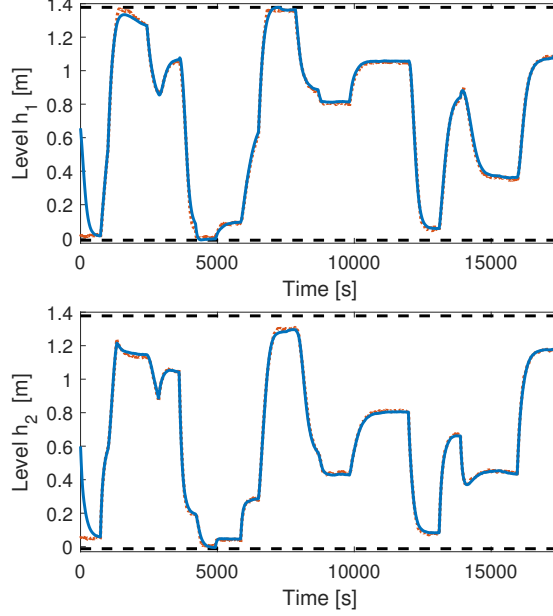
13

Figure 6: Performances of the trained model on an independent test set: GRU open-loop prediction (blue line) compared to the measured output (red dotted line). Level h_1 is displayed on top, level h_2 on the bottom.

5.3. Feasible set-points generation

After learning the model, the dataset used to train the controller network $\mathcal{C}$ has been generated. As discussed in Section 3.2, this dataset consists in a set of reference trajectories that the controller should learn to track – no data needs to be collected from the real system at this stage. These reference trajectories are rather obtained by filtering MPRB signals, denoted by y^0, with the reference model $\mathcal{M}_r$, herein chosen as the discrete-time equivalent of a pair of decoupled first-order systems with unitary static gain and time constant $\tau_r = 2000s$.

For successful controller training, the dataset must be properly generated. Indeed, the inclusion of unfeasible set-points $y^0(k)$, i.e. set-points which (given the constraints on the inputs) do not correspond to any feasible equilibrium of the model, would inevitably alter the loss function's gradient, leading to poor performances of the trained controller.

In light of the model's δISS, checking the existence of an input sequence that steers the model to the set-point reduces to assess the existence of some feasible constant input u_s and some state $\xi_s \in \Xi$ such that (u_s, ξ_s, y^0) is an equilibrium of the model, i.e.

$$\begin{cases} \xi_s = f_m(\xi_s, u_s, \Phi_m^*) \\ y^0 = g_m(\xi_s, \Phi_m^*) \end{cases}. \tag{18}$$

Moreover, the δISS property guarantees that, if such u_s exists, it is unique and that the equilibrium (u_s, ξ_s, y^0) can be reached from any initial state of the model. Hence, this
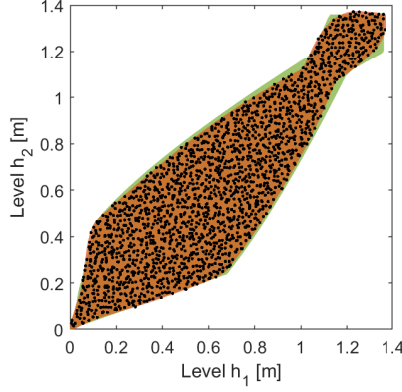
Figure 7: Controller dataset generation: set-points (black dots) are extracted from the set of model's feasible outputs (orange area); the green area corresponds to the set of plant's feasible outputs, generally unknown.

property further allows to relieve the computational complexity of solving (18), since initial guesses of u_s and ξ_s – to be used for warm-starting the nonlinear solver – can be easily retrieved from open-loop simulations of (7).

Overall, $N_s = 430$ reference trajectories $\boldsymbol{y}^{0,\{i\}}$ with length $T_s^{\{i\}} = 600$ have been generated, 380 of which used for training, 40 used for validation, and 10 for the final testing. Each reference trajectory consists in sequences of random steps which satisfy the aforementioned feasibility condition. In Figure 7 the extracted random set-points are compared to the set of feasible model outputs, and to the set of feasible plant outputs. This latter is generally unknown, and is here reported just for comparison purposes. The MPRB references are then filtered with the model reference $\mathcal{M}_r$ to obtain the reference trajectories $\tilde{\boldsymbol{y}}^{0,\{i\}}$, used for the training of the controller network.

5.4. Controller training

The controller is learned by a deep GRU with $M = 3$ layers, each one featuring $n_i = 5$ units. The training procedure proposed in Section 3.2 has been carried out with TensorFlow 1.15, using RMSProp as optimizer. As for the training of the model, the δISS property of the controller network has been enforced using a piece-wise linear cost $\rho(\nu^i)$ which penalizes the violation of the δISS condition (5).

At each epoch of the training procedure, the set of references is randomly divided into batches, with respect to which the optimizer tunes the weights of the controller network. After each epoch, the performance metrics have been evaluated on the validation set, and the training was halted when they stop improving. The evolution of the loss function throughout the training procedure is shown in Figure 8. Overall, the controller training took 1543 epochs. Eventually, the controller's performances have been tested on the independent test-set's reference trajectories. The results on one of these test references is depicted in Figure 9. Note that, in addition to limited steady-state tracking errors, cross-coupling effects between the two outputs are present. Despite these effects which, although promptly compensated, may deteriorate the FIT index, a remarkable $FIT = 87\%$ is scored for the reported test reference trajectory.
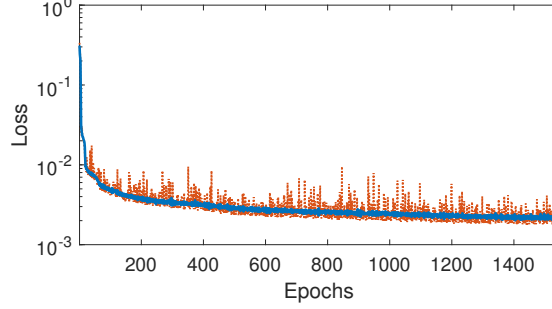
15

Figure 8: Controller training: evolution of the average loss function across all the batches (blue line) and MSE on the validation dataset (red dotted line).
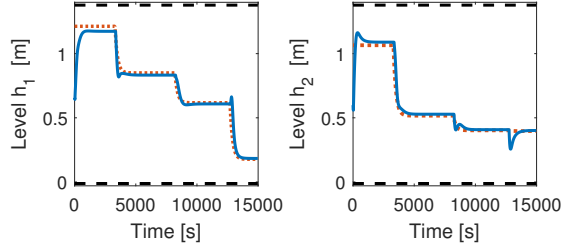

Figure 9: Performances of the controller on a reference trajectory extracted from the independent test set: reference (red dotted line) versus controlled output (blue line). The level h_1 is displayed on the left, the level h_2 on the right.
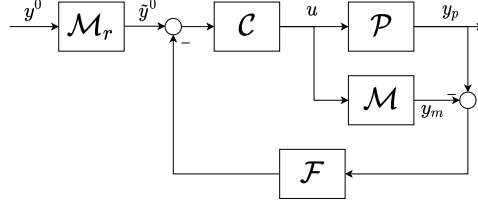

Figure 10: IMC architecture with filtered modeling error feedback.

5.5. Closed-loop performances

Eventually, the closed-loop performances of the proposed control architecture have been tested on the simulated Quadruple Tank system, where the outputs have been corrupted by a white Gaussian noise with standard deviation 0.02.

To cope with the measurement noise, the modified architecture shown in Figure 10 has been considered, where the modeling error feedback e_m is customarily filtered by a low-pass filter. In particular, we adopted a low-pass filter $\mathcal{F}$ with the same time constant as the model reference, i.e. τ_r. In this way, the architecture reported in Figure 10 is the analogous to the one proposed in [21]. It is worth noticing that the low-pass filter does not affect the closed-loop stability. Indeed, the modeling error feedback e_m acts as an additive disturbance on the reference $\tilde{y}^0$ [21], and it converges to the bounded plant-model mismatch (or to zero, in the case of perfect model), see Section 4.
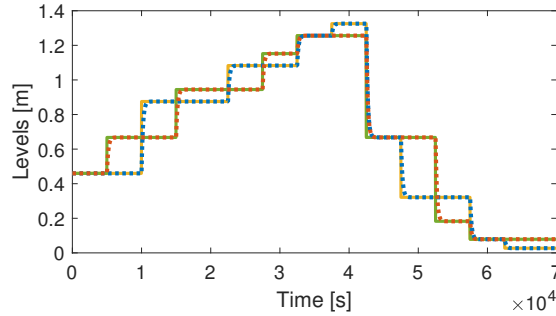
16

Figure 11: Reference trajectories used for testing the closed-loop performances. The step references y^0 are the continuous lines (yellow and green, respectively), while the filtered references $\tilde{y}^0$ are represented as dotted lines (blue and red, respectively).

The closed-loop performances have been tested using the reference trajectories shown in Figure 11, so as to span the set of model's feasible steady-states, see again Figure 7. As depicted in Figure 12, remarkable closed-loop performances are achieved. As expected, cross-couplings are promptly rejected and the controlled outputs are kept close to their reference values, while the controller's architecture allows to satisfy the input saturation constraint, as illustrated in Figure 13.

The same output references have also been tested in noise-free conditions, in order to quantify the closed-loop tracking performances. In this case, the average steady-state tracking error is $2 \cdot 10^{-3}$, while the maximum steady-state tracking error is 0.023.

Note that, in applications where offset-free tracking is required, integrators – equipped with suitable anti-windup mechanisms – can be placed on the output tracking errors. This configuration has also been tested in [32], where it allowed to achieve offset-free tracking for most references, provided that a careful selection of the integrators' gains is performed to avoid adverse effects on the closed-loop stability.

6. Conclusion

In this paper, we discussed how Recurrent Neural Networks, particularly Gated Recurrent Units (GRUs), can be employed to design an Internal Model Control (IMC) architecture to control a stable nonlinear dynamical system. The system model retrieval and the model inversion were recast as standard RNNs' training procedures. Moreover, recent GRUs' stability results were exploited to guarantee the stability of both the model and the controller to guarantee the closed-loop stability. The approach was tested on the Quadruple Tank benchmark system, showing good closed-loop performances and inputs' constraint satisfaction. Future work will be devoted to the use of integrators to attain robust offset-free tracking capabilities.
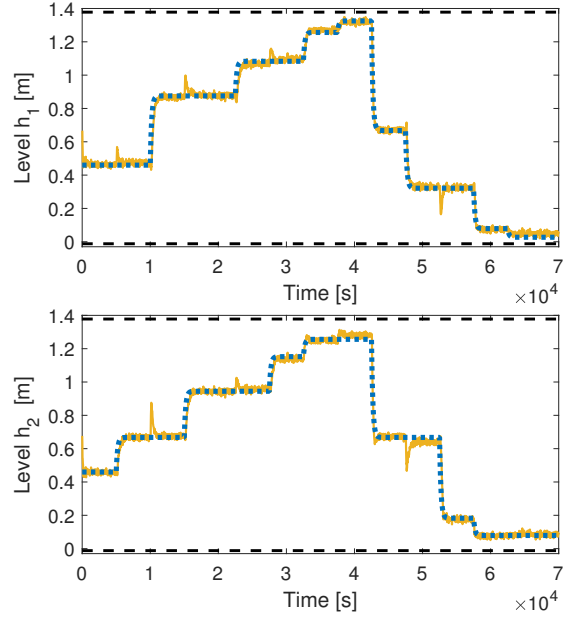
Acknowledgments

17

Figure 12: Plant's outputs (yellow continuous lines) compared to their reference values (blue dotted lines) and to the minimum and maximum values (black dashed lines). Level h_1 is displayed on top, level h_2 on the bottom.
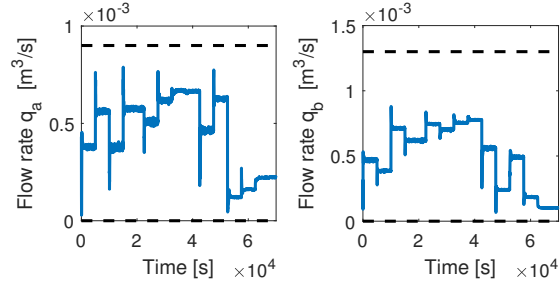

Figure 13: Denormalized control variables (q_a on the left, q_b on the right) compared to their minimum and maximum values (black dashed-dotted lines).

18

References

[1] M. Forgione, D. Piga, Model structures and fitting criteria for system identification with neural networks, in: 2020 IEEE 14th International Conference on Application of Information and Communication Technologies (AICT), IEEE, 2020, pp. 1–6.

[2] A. Rehmer, A. Kroll, On using gated recurrent units for nonlinear system identification, in: 2019 18th European Control Conference (ECC), IEEE, 2019, pp. 2504–2509.

[3] K. J. Hunt, D. Sbarbaro, R. Żbikowski, P. J. Gawthrop, Neural networks for control systems—a survey, Automatica 28 (6) (1992) 1083–1112.

[4] J. M. Ali, M. A. Hussain, M. O. Tade, J. Zhang, Artificial intelligence techniques applied as estimator in chemical process systems–a literature survey, Expert Systems with Applications 42 (14) (2015) 5915–5931.

[5] Y. Bengio, I. Goodfellow, A. Courville, Deep learning, Vol. 1, MIT press Massachusetts, USA, 2017.

[6] K. Hornik, M. Stinchcombe, H. White, et al., Multilayer feedforward networks are universal approximators., Neural networks 2 (5) (1989) 359–366.

[7] F. M. Bianchi, E. Maiorino, M. C. Kampffmeyer, A. Rizzi, R. Jenssen, Recurrent neural networks for short-term load forecasting: an overview and comparative analysis, Springer, 2017.

[8] W. Yu, Nonlinear system identification using discrete-time recurrent neural networks with stable learning algorithms, Information sciences 158 (2004) 131–147.

[9] O. Ogunmolu, X. Gu, S. Jiang, N. Gans, Nonlinear systems identification using deep dynamic neural networks, arXiv preprint arXiv:1610.01439 (2016).

[10] A. M. Schäfer, H. G. Zimmermann, Recurrent neural networks are universal approximators, in: International Conference on Artificial Neural Networks, Springer, 2006, pp. 632–640.

[11] S. Hochreiter, The vanishing gradient problem during learning recurrent neural nets and problem solutions, International Journal of Uncertainty, Fuzziness and Knowledge-Based Systems 6 (02) (1998) 107–116.

[12] J. Chung, C. Gulcehre, K. Cho, Y. Bengio, Empirical evaluation of gated recurrent neural networks on sequence modeling, arXiv preprint arXiv:1412.3555 (2014).

[13] S. Hochreiter, J. Schmidhuber, Long short-term memory, Neural computation 9 (8) (1997) 1735–1780.

[14] M. A. Hosen, M. A. Hussain, F. S. Mjalli, Control of polystyrene batch reactors using neural network based model predictive control (NNMPC): An experimental investigation, Control Engineering Practice 19 (5) (2011) 454–467.

[15] W. Wong, E. Chee, J. Li, X. Wang, Recurrent neural network-based model predictive control for continuous pharmaceutical manufacturing, Mathematics 6 (11) (2018) 242.

[16] N. Lanzetti, Y. Z. Lian, A. Cortinovis, L. Dominguez, M. Mercangöz, C. Jones, Recurrent neural network based MPC for process industries, in: 2019 18th European Control Conference (ECC), IEEE, 2019, pp. 1005–1010.

[17] Z. Wu, A. Tran, D. Rincon, P. D. Christofides, Machine learning-based predictive control of nonlinear processes. Part I: Theory, AIChE Journal 65 (11) (2019) e16729.

[18] K. Patan, Neural network-based model predictive control: Fault tolerance and stability, IEEE Transactions on Control Systems Technology 23 (3) (2014) 1147–1155.

[19] E. Terzi, F. Bonassi, M. Farina, R. Scattolini, Learning model predictive control with long short-term memory networks, International Journal of Robust and Nonlinear Control (2019). doi:https://doi.org/10.1002/rnc.5519.

[20] F. Bonassi, C. F. O. da Silva, R. Scattolini, Nonlinear MPC for Offset-Free Tracking of systems learned by GRU Neural Networks, in: 3rd IFAC Conference on Modelling, Identification and Control of Nonlinear Systems (MICNON 2021), 2021.

[21] C. G. Economou, M. Morari, B. O. Palsson, Internal model control: Extension to nonlinear system, Industrial & Engineering Chemistry Process Design and Development 25 (2) (1986) 403–411.

[22] M. Morari, E. Zafiriou, Robust process control, Morari, 1989.

[23] K. Hunt, D. Sbarbaro, Neural networks for nonlinear internal model control, in: IEE Proceedings D (Control Theory and Applications), Vol. 138, IET, 1991, pp. 431–438.

[24] I. Rivals, L. Personnaz, Nonlinear internal model control using neural networks: Application to processes with delay and design issues, IEEE transactions on neural networks 11 (1) (2000) 80–90.

[25] F. Bonassi, M. Farina, R. Scattolini, Stability of discrete-time feed-forward neural networks in NARX configuration, in: 19th IFAC Symposium on System Identification (SYSID 2021), 2021.

[26] F. Bayer, M. Bürger, F. Allgöwer, Discrete-time incremental ISS: A framework for robust NMPC, in: 2013 European Control Conference (ECC), IEEE, 2013, pp. 2068–2073.

[27] F. Bonassi, E. Terzi, M. Farina, R. Scattolini, LSTM neural networks: Input to state stability and probabilistic safety verification, in: Learning for Dynamics and Control, 2020, pp. 85–94.

[28] F. Bonassi, M. Farina, R. Scattolini, On the stability properties of Gated Recurrent Units neural networks, arXiv preprint arXiv:2011.06806 (2020).

[29] D. M. Stipanović, M. N. Kapetina, M. R. Rapaić, B. Murmann, Stability of gated recurrent unit neural networks: Convex combination formulation approach, Journal of Optimization Theory and Applications (2020) 1–16.

[30] I. Alvarado, D. Limon, D. M. De La Peña, J. M. Maestre, M. Ridao, H. Scheu, W. Marquardt, R. Negenborn, B. De Schutter, F. Valencia, et al., A comparative analysis of distributed MPC techniques applied to the HD-MPC four-tank benchmark, Journal of Process Control 21 (5) (2011) 800–815.

[31] R. Pascanu, T. Mikolov, Y. Bengio, On the difficulty of training recurrent neural networks, in: International conference on machine learning, 2013, pp. 1310–1318.

[32] L. Depari, Design of internal model control systems with recurrent neural networks, Master thesis, Politecnico di Milano, Supervisors: F. Bonassi, R. Scattolini. (2021).